6ICEGE
6th International Conference on Earthquake Geotechnical Engineering
1-4 November 2015
Christchurch. New Zealand

Comparison of Two Simplified Methods to Evaluate the Performance of Three Pile-Supported Bridges Affected by Liquefaction during the 2010 Maule Earthquake

C. Ledezma[1], D. Gonzalez[2], A. Gutierrez[3]

ABSTRACT

Recent earthquakes have showed that the interaction between laterally spreading ground and structures with deep foundations is still far from being completely understood. During the 2010 M8.8 Maule earthquake, several pile-supported bridges were affected by this phenomena causing different levels of damage. Among these bridges, three were selected because clear evidence of liquefaction was observed at their respective locations, and also because their seismic performance was very different, ranging from little (Mataquito Bridge) to moderate (Llacolen Bridge) to large foundation deformations (Juan Pablo II Bridge). This article presents a comparison of two simplified methods to evaluate the seismic performance of these bridges. The first one is a modified version of the simplified design procedure proposed in the MCEER/ATC-49-1 report were the residual lateral displacement is estimated by means of intersecting two curves: one that represents the lateral force-displacement curve of the structure stabilizing the sliding soils mass, and one that corresponds to the estimated residual displacements of the soil mass for different levels of restraining force. The second method is based on a numerical model where after static equilibrium is reached (pre-earthquake condition) liquefied properties are assigned to those layers with high liquefaction potential (post-earthquake condition), and the model is run until equilibrium is reached once again (inertial effects are neglected). Reasonable agreement was found between these two models for the case of Mataquito and Llacolen, and some preliminary conclusions are drawn from the performed analyses.

Introduction

In this paper, three case-histories of bridges investigated by the Geotechnical Extreme Events Reconnaissance (GEER) teams during several visits after the 2010 M8.8 Maule earthquake are presented. The observations provided herein are based on the GEER edited report (Bray et al., 2010) and on Ledezma et al. (2012).

Two of the three bridges presented in this paper cross the Bío-Bío River, which is the second longest river in Chile. It is also the widest river in Chile, with an average width of 1 km, and a width of more than 2 km prior to discharging into the ocean. Close to the Pacific Ocean, the river traverses the metropolitan area of Concepción, Chile's second largest metropolitan area. In Concepción, the river is crossed by five bridges. The ones that were analyzed were: Llacolén

[1]Assistant Professor, Structural and Geotechnical Engineering Department, Pontificia Universidad Catolica de Chile, Santiago, Chile, cledezma@ing.puc.cl
[2]Graduate Student, Structural and Geotechnical Engineering Department, Pontificia Universidad Catolica de Chile, Santiago, Chile, dvgonzalez@uc.cl
[3]Graduate Student, Structural and Geotechnical Engineering Department, Pontificia Universidad Catolica de Chile, Santiago, Chile, aegutier@uc.cl

Bridge (opened in 2000) and Juan Pablo II Bridge (1974). The third analyzed bridge is the Mataquito Bridge (2006), located near Iloca (to the north of the epicenter area). During the 2010 Maule earthquake, all of these bridges experienced different levels of structural damage, compromising normal business activities in the region. The most common geotechnical failure mechanism observed at these bridges was liquefaction-induced lateral spreading that occurred along both shores of the Bío-Bío River and Mataquito River. Lateral spreading contributed to the approach fill deformations.

Liquefaction Susceptibility

Liquefaction susceptibility was evaluated at the three bridge sites using the Standard Penetration Test (SPT) profiles obtained before and after the earthquake, which were provided by the Ministry of Public Works (MOP). The sand liquefaction triggering procedure presented in Youd et al. (2001) was used to define an approximate normalized SPT threshold value for the occurrence of liquefaction. The 2010 Maule earthquake had a moment magnitude of Mw=8.8, and the ground motion had a peak ground acceleration of PGA≈0.4g in both areas, Concepcion and Iloca (R≈100 km from the epicenter) (Boroschek et al., 2010).

Liquefaction Effects

Effects of liquefaction-induced lateral spreading were evaluated using two approaches.

The first approach (called Method 1 in this article) is based on the simplified design procedure proposed in the MCEER/ATC-49-1 recommended seismic design document of bridges. Some of the principal steps involved in this design procedure are:

- Identify the soil layers that are likely to liquefy. A boring located near the area of interest for each bridge was selected and evaluated according to the sand liquefaction triggering procedure presented in Youd et al. (2001).
- Assign undrained residual strengths S_{ur} to the layers that liquefy. The post-liquefaction S_{ur} strength was evaluated using the expression recommended in Ledezma and Bray (2010).
- Perform pseudo-static seismic stability analysis to calculate the yield coefficient (k_y) for the critical potential sliding mass. For all the cases, the horizontal force P required to reach a factor of safety (FS) of 1.0 was calculated for horizontal accelerations k_h of 0.05, 0.10, 0.15, 0.20, 0.25, 0.30, and 0.35. Therefore $k_y = k_h$ since FS=1.0.
- Estimate the maximum lateral ground displacement. The Bray and Travasarou relationship (Bray and Travasarou, 2007) was used to estimate the lateral displacement associated with each horizontal acceleration. The initial fundamental period of the sliding mass (Ts) was estimated using the expression: $T_s = 4H/V_s$, where H = the average height of the potential sliding mass, and V_s is the average shear wave velocity of the sliding mass. Shear wave velocities were estimated using the V_s versus N-SPT correlations proposed by Bellana (2009). Additional considerations for this analysis were Mw=8.8 and $S_a(1.5T_s)$=0.4g.
- Identify the plastic mechanism that is likely to develop as the ground displaces laterally. A simple elasto-plastic model is used to reproduce the pile behavior.
- From an analysis of the pile response to a liquefaction-induced ground displacement field, the likely shear resistance of the foundation is estimated. A pushover analysis for each case

was performed. Each model was developed in a software for laterally loaded piles, LPile v2012 (ENSOFT). All models consider a single-pile geometry and the same soil profile properties assumed in the slope stability model. Several assumptions and modeling options were considered to establish a range of possible solutions for the compatible force-displacement state from the pushover analysis and the slope lateral deformation. Four different types of p-y curve models were used to represent the liquefied layer, and two were used for the non-liquefied layer. The p-y curve for sands recommended in Reese et al. (1974) and the p-y curves proposed in O'Neill and Murchinson (1983), included in the American Petroleum Institute RP 2A-WSD, were used in both layers. The p-y curves for liquefied sands presented in Rollins et al. (2005) and the p-y curves for soft clays from Matlock (1970) were used in the liquefied layer, in addition to the sand curves mentioned before.

The second method (called Method 2 in this paper) is based on a numerical model where after static equilibrium is reached (pre-earthquake condition) liquefied properties are assigned to those layers with high liquefaction potential (post-earthquake condition), and the model is run until equilibrium is reached once again (inertial effects are neglected). The bridge models were created using the software FLAC2D V7.0 focusing on what happened at the abutments. The geometry and the structural properties were obtained from the construction drawings provided by the Ministry of Public Works. The Mohr-Coulomb soil model was used in the numerical models, and the soil properties (bulk and shear modulus, friction angle, and densities) were estimated from SPT correlations. The post-earthquake residual undrained shear strength of the liquefiable layers was estimated using the recommendations by Ledezma and Bray (2010). In FLAC, these residual strengths were included as an equivalent cohesion with dependence on the effective vertical stress. The pile group foundation system was modeled using equivalent properties and FLAC's pile elements, along with shear and normal springs to represent the interaction between the piles and the surrounding soil.

Considerations for Pile Response Analysis

For both types of analyses, and based on the structural drawings provided by MOP, the piles and piers were modeled considering a compressive strength of $f_c' = 25MPa$ for the concrete, and yield and ultimate stresses for the steel of $f_y = 420MPa$ and $f_u = 630MPa$, respectively. These nominal properties were respectively modified by factors $R_c=1.3$, $R_y=1.2$ and $R_u=1.2$ to represent the actual in-situ strength of the piles at the time of the earthquake. These factors are based in the ACI and AISC recommendations.

Mataquito Bridge

Liquefaction Susceptibility

The Mataquito Bridge is a 320 m-long, 8-span, reinforced concrete structure that crosses the Mataquito River close to the Pacific Ocean. Each abutment of this bridge was supported by two rows of four drilled shafts of circular section. The boring S-1A located near the south abutment was selected for liquefaction evaluation. This evaluation showed that the presence of liquefied material was confined to the upper 5 meters of the soil deposit (Fig. 3). Given that the piles' length was ~17 meters, approximately more than half of the length was embedded. This probably

provided enough vertical and lateral support for the piles to resist the vertical and lateral loads, despite the occurrence of liquefaction at shallow depths. An average value of $(N_1)_{60cs}$ ≈9 blows/ft was estimated for the full depth of the liquefied layer. Following the recommendations in Ledezma and Bray (2010), the calculated $\overline{S_{ur}}/\sigma_v'$ ratio for the both models was 0.096.

Results from Method 1

After creating a slope stability model of Mataquito Bridge's south abutment, the required lateral force to get FS=1 for different horizontal accelerations is calculated. Then, the Bray and Travasarou (Bray and Travasarou, 2007) relationship is used to get the lateral force versus displacement curves. Figure 1 shows that the resulting curve depends on the slope stability procedure that is used. Also, this figure includes the 16% and 84% percentiles from the Bray and Travasarou relationship. Then, a pushover analysis is performed considering an equivalent single-pile geometry and the aforementioned soil properties. Given that at each abutment there were two rows of piles along the transverse direction of the bridge, considering a spacing of S = 4 m between piles, and that V is the shear force in the pile, the equivalent per-unit-width force R was estimated as R = 2V/S. The estimated residual lateral displacement can be found at the intersection of these curves. This simplified approach estimates residual lateral displacements at the south abutment in the range of 4 to 10 cm, but they can be as high as ~18 cm, which is a conservative estimate when compared to what was observed in the field (Fig. 1).

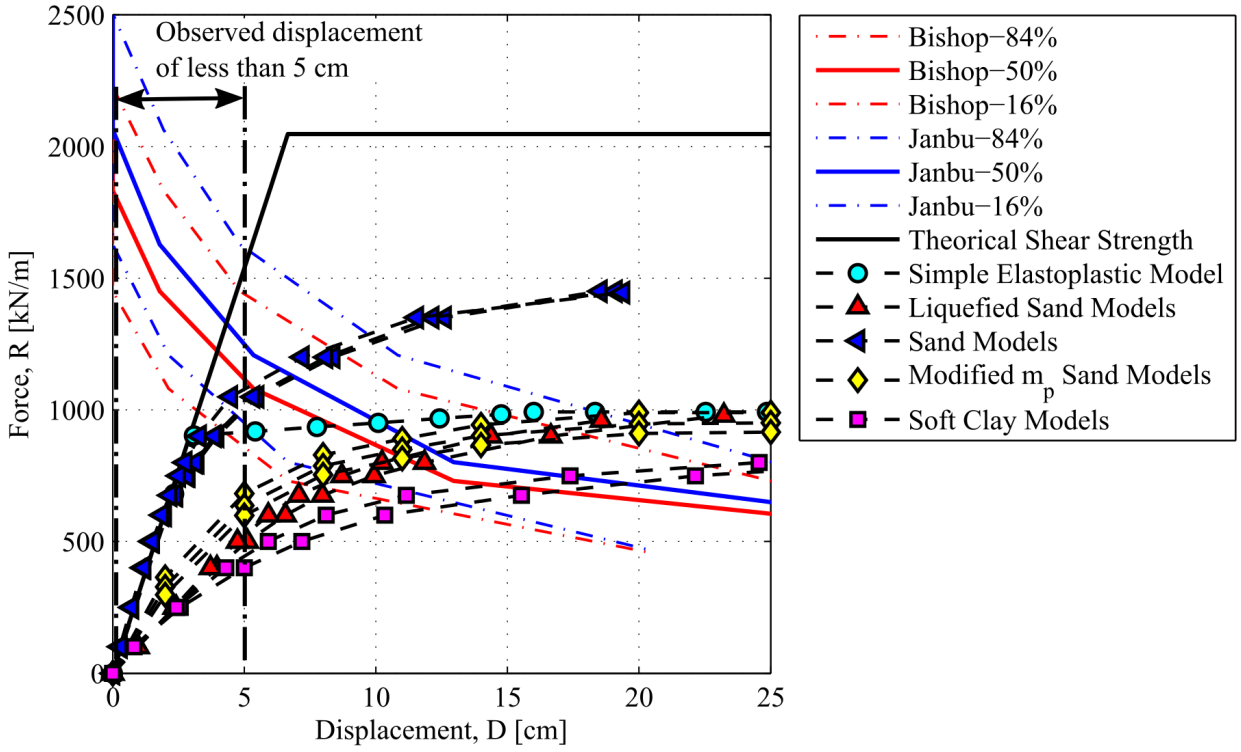

Figure 1. Expected lateral displacement D for different values of the resisting force R for the piles in the south abutment of the Mataquito Bridge (different p-y curves were used).

Results from Method 2

The model considered an equivalent pile geometry with two rows of piles in the south abutment, with a center-to-center spacing of 4 m between piles. Figures 2 and 3 show, respectively, the calculated lateral pile displacements and bending moments, on top of the deformed mesh.
These analyses show that the maximum displacement, of about 1 cm (in concordance with field observations), is located at the top of the piles. However, the soil settlements near the row of piles closest to the river, of ~0.5 m-1.0 m, are higher than those observed in the field, probably due to the small residual shear strength that was assigned to the layers that liquefied near the surface. On the other hand, the bending moment shows a sign change close to the middle of the liquefied layer, and it has a maximum of around 20% of the maximum moment capacity.

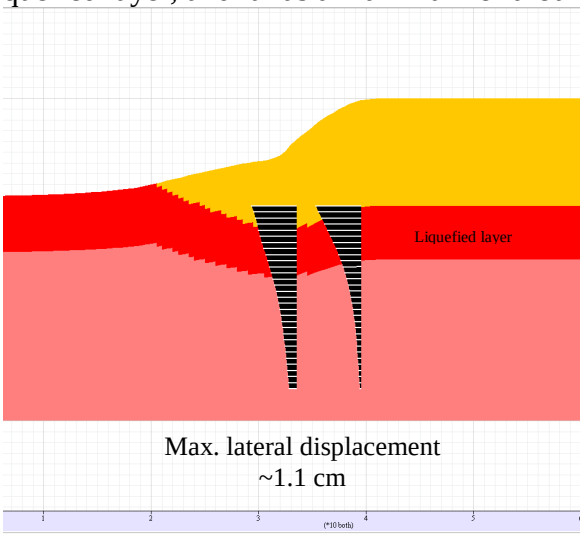

Figure 2. Lateral displacement profile for the piles in the south abutment of Mataquito Bridge. Post-earthquake condition.

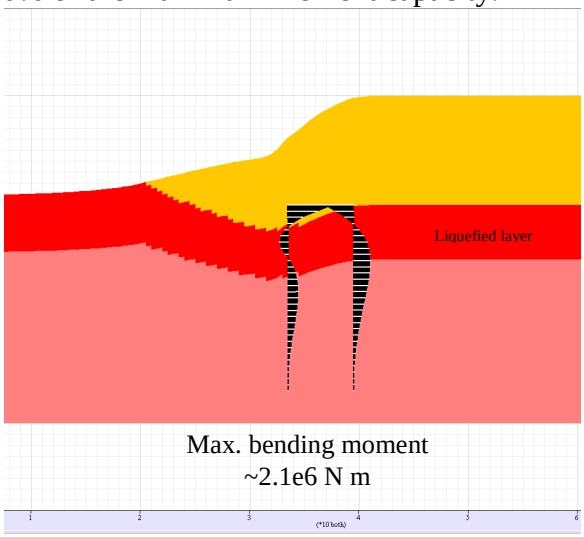

Figure 3. Bending moment profile for the piles near the north abutment of Mataquito Bridge. Post-earthquake condition.

Juan Pablo II Bridge

Liquefaction Susceptibility

The Juan Pablo II Bridge is the longest vehicular bridge in Chile, spanning 2,310 m in length. The bridge was opened in 1974. The bridge consists of 70 spans (length = 33 m, width = 21.8 m). Each span sits on reinforced concrete bents with drilled pile supports, piles' length was ~16 meters. Column shear failure, vertical displacements of the bridge deck, and rotation of the bridge bent of 1° to 3° occurred at the northeast approach. In contrast with the damage observed at the northeast approach, the southwest approach suffered minor damage. Boring S-14 located near the north abutment and to pier No. 66 was selected for liquefaction evaluation. Following the procedure used in the Mataquito Bridge, distinct layers of liquefiable material were observed and, according to our analyses, the soil below the tip of the piles likely liquefied during this event. Three liquefied layers were defined, with thicknesses of 6 m, 3 m and 5 m. Average values of $(N_1)_{60cs}$ were estimated for the full depth of each liquefied layer. The average $(N_1)_{60cs}$ values were 14, 10 and 12.5 blows/ft, following the recommendations in Ledezma and

Bray (2010), and the calculated $\overline{S_{ur}}/\sigma_v'$ ratios for both models were 0.20, 0.11 and 0.16 respectively.

Results from Method 1

After creating a slope stability model of Juan Pablo II's north end, the required lateral force to get FS=1 for different horizontal accelerations is calculated. Then, the Bray and Travasarou (Bray and Travasarou, 2007) relationship is used to get the lateral force versus displacement curves. A pushover analysis of bent column No. 66 was performed. Since the shear failure occurred in the column, and the sequence of liquefiable and non-liquefiable layers did not seem to provide enough lateral restraint, the pushover analysis focused on the column rather than on the piles. The model considered an equivalent single pile and column geometry, and the same soil profile properties assumed in the slope stability model. In this case, there was only one row of columns and piles along the transverse direction of the bridge, considering a spacing of S = 13 m between piles, the equivalent per-unit-width force R was estimated as R = V/S, were V is the shear force in the pier. This simplified analysis shows that the expected lateral displacement at this bent (>10 cm) is consistent with the shear failure of the supporting column observed in the field (Fig. 4).

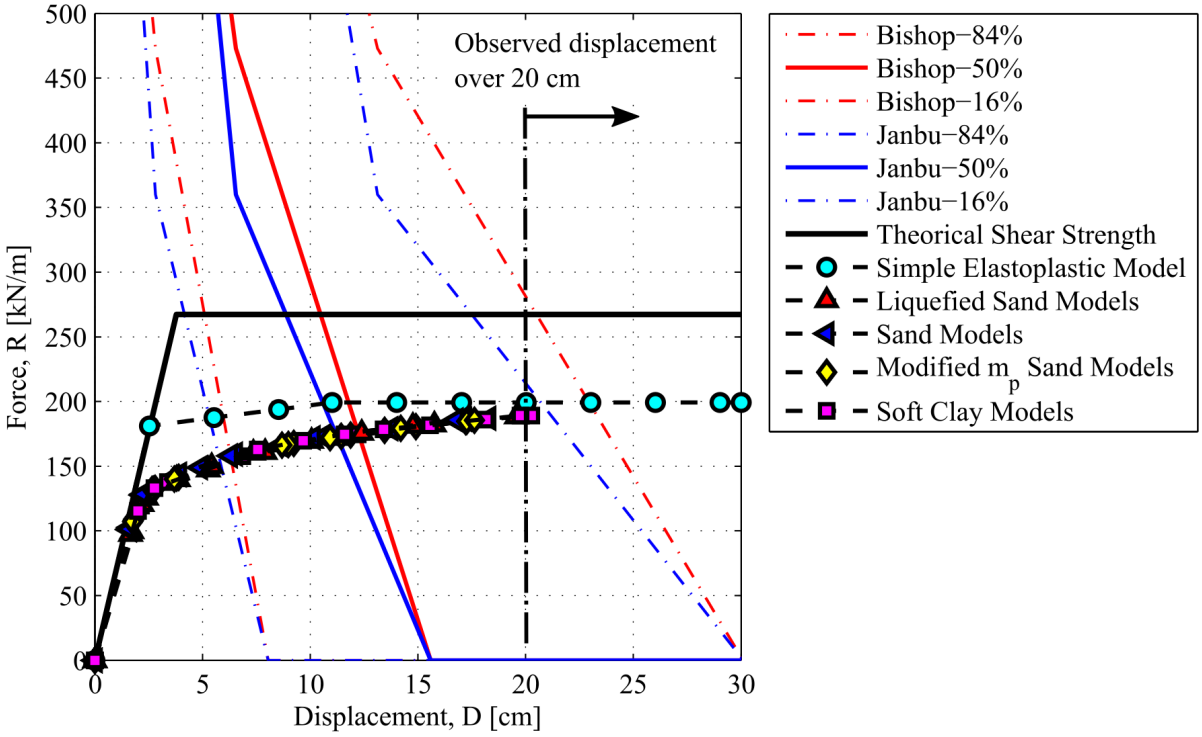

Figure 4. Expected lateral displacement D for different values of resisting force R for the columns of Pier No. 66 near the north abutment of Juan Pablo II Bridge (different p-y curves were used).

Results from Method 2

The pile foundations was modeled using an equivalent pile-column geometry. Figures 5 and 6 show, respectively, the calculated lateral pile displacement and the bending moment profiles on top of the deformed mesh.

These results indicate that the maximum displacement, of about 0.4 cm, takes place in the first liquefiable layer level, which does not agree with what was observed in the field. Different modeling strategies are currently being evaluated to better represent the field observations. Figure 6 shows that the maximum bending moment takes place in the upper liquefied zone, and it reaches ~25% of the maximum bending capacity of the column. The corresponding mobilized shear strength of the column was ~27% of its maximum capacity.

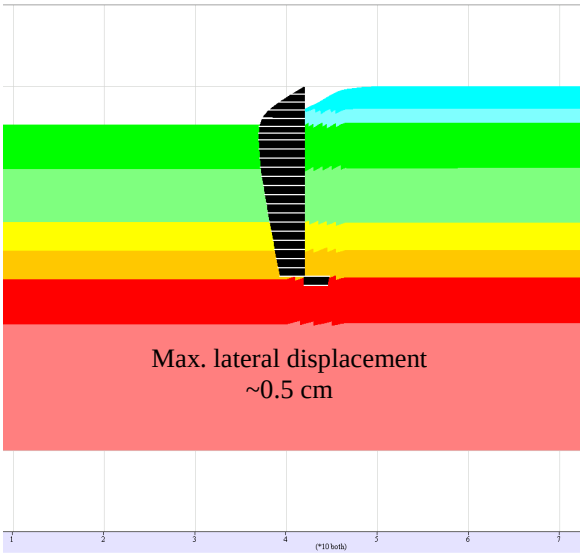

Figure 5. Lateral displacement profile for the piles near the north abutment of Juan Pablo II Bridge. Post-earthquake condition.

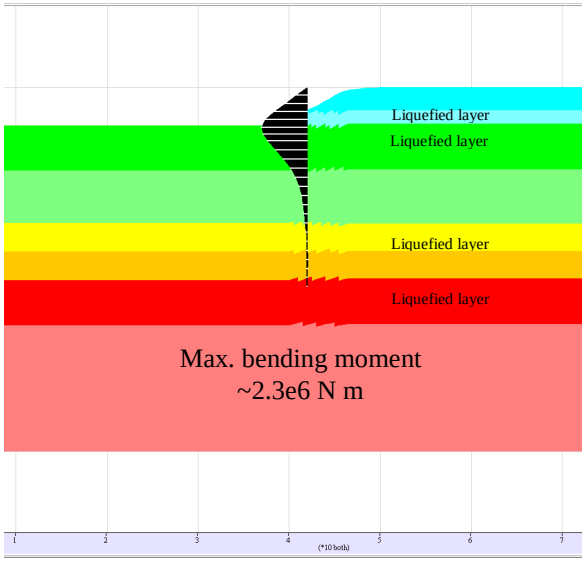

Figure 6. Bending moment profile for the piles near the north abutment of Juan Pablo II Bridge. Post-earthquake condition.

Llacolen Bridge

Liquefaction Susceptibility

The Llacolén Bridge in Concepción was constructed in the year 2000 and it spans 2,160 m across the Bío-Bío River. The bridge is a multispan, simply supported concrete girder bridge. In contrast to the Juan Pablo II Bridge, the average piles' length in the Llacolén Bridge was ~20 m. During the earthquake, lateral spreading at the northeast approach unseated the bridge deck at its shoreline support, forcing closure of the bridge until a temporary deck could be erected. Boring S-6 located near the north abutment and to pier No. 48 was selected for liquefaction evaluation. Distinct layers of liquefiable material were observed after the liquefaction evaluation. Unlike Juan Pablo II Bridge the soil below the tip of the piles likely did not liquefy during this event. Three liquefied layers were defined, with thicknesses of 2 m, 3 m and 7.5 m. Average values of

$(N_1)_{60cs}$ were estimated for the full depth of each liquefied layer. The average $(N_1)_{60cs}$ values were 8.7, 10.8 and 12.5 blows/ft, following the recommendations in Ledezma and Bray (2010), the calculated $\overline{S_{ur}}/\sigma_v{}'$ ratios for both models were 0.09, 0.13 and 0.23 respectively.

Results from Method 1

The slope stability analyses were similar to the ones performed for the Mataquito and Juan Pablo II Bridges. Pushover analyses of Llacolén Bridge's were performed for Bent No. 48 considering different p-y models. It was assumed that the connection of the piers to the bridge deck did not provide enough fixity against rotation, so the piles were the only elements restraining the lateral movement of the sliding soil mass. The model considered an equivalent single-pile geometry and the same soil profile properties assumed in the slope stability model. Similar to the Juan Pablo II bridge case, the bents had only one row of columns and piles along the transverse direction of the bridge, considering a spacing of S = 4.81 m between piles, the equivalent per-unit-width force R was estimated as R = V/S, were V is the shear force in the pile. This simplified analysis shows that the expected residual lateral displacement at this abutment (2 to 5 cm) is consistent with the small to moderate residual lateral displacements observed in the field, which do not fully explain the deck collapse (Fig. 7).

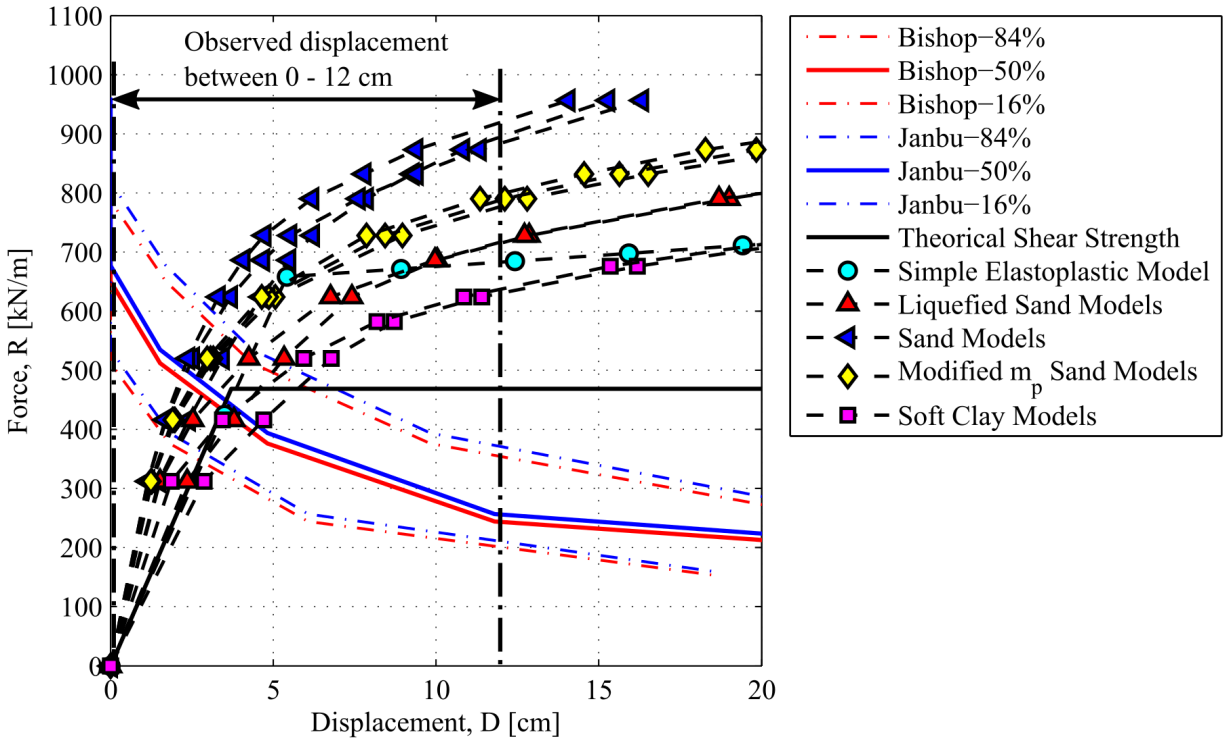

Figure 7. Expected lateral displacement D for different values of resisting force R for the piers of Pier No. 48 near the north abutment of Llacolén Bridge (different p-y curves were used).

Results from Method 2

The model considered an equivalent single-pile geometry with a spacing of 4.5 m between piles (or columns). Figures 8 and 9 show, respectively, the calculated lateral displacement and bending moment profiles on top of the final deformed mesh.
This analysis shows that the maximum displacement, of about 1.2 cm, is located at the top of the upper liquefied layer, which compares well with that observed in the field (Figure 8).
The bending moment shows a sign change between the upper non-liquefied layer and the second from the top liquefied layer, and it has a maximum of about 40% of the total capacity.

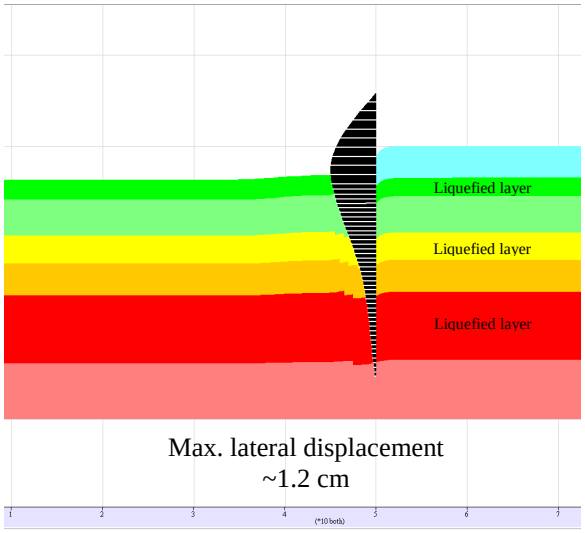

Figure 8. Lateral displacement profile for the piles near the north abutment of Llacolén Bridge. Post-earthquake condition.

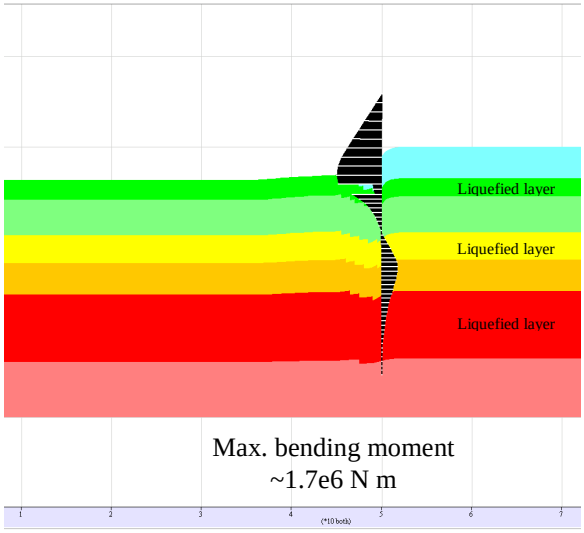

Figure 9. Bending moment profile for the piles near the north abutment of Llacolén Bridge. Post-earthquake condition.

Conclusions

The results of two simplified methods to evaluate the seismic performance of the Mataquito, Juan Pablo II, and Llacolen bridges are compared. In the first method the residual lateral displacement is estimated by means of intersecting two curves: one that represents the lateral force-displacement curve of the structure stabilizing the sliding soils mass, and one that corresponds to the estimated residual displacements of the soil mass for different levels of restraining force. The second method is based on a numerical model where after static equilibrium is reached, liquefied properties are assigned to those layers with high liquefaction potential, and the model is run until equilibrium is reached again (inertial effects are neglected). Reasonable agreement was found between these two methods for the case of Mataquito and Llacolen, but nor for the case of Juan Pablo II. Different modeling strategies are now being evaluated to try to explain these differences. Regarding the Llacolen Bridge case, both methods agree on that the deck collapse cannot be explained by kinematics effects only.

Acknowledgments

This research was made possible by grants from the Chilean National Commission for Scientific and Technological Research under Fondecyt de Iniciación Award Number 11110125. The authors would also like to thank Carla Serrano, MS student at the Pontificia Universidad Católica de Chile, for compiling the SPT data that was used for this study, and also to the Ministry of Public Works (MOP, Chile) for providing the required data to perform the analyses.

References

Bray JD and Frost JD, Eds. *Geo-engineering Reconnaissance of the 2010 Maule, Chile Earthquake*, a report of the NSF- Sponsored GEER Association Team, primary authors: Arduino et al. 2010 http://www.geerassociation.org/.

Ledezma C, Hutchinson T, Ashford S, Moss RES, Arduino P, Bray JD, Olson SM, Hashash Y, Verdugo R, Frost D, Kayen R, and Rollins L. Effects of Ground Failure on Bridges, Roads, and Railroads. *Earthquake Spectra* 2012; **28** (S1): S119-S143.

Youd TL, Idriss IM, Andrus RD, Arango I, Castro G, Christian JT, Dobry R, Liam Finn WD, Harder Jr. LF, Hynes ME, Ishihara K, Koester JP, Liao S, Marcuson III WF, Martin GR, Mitchell JK, Moriwaki Y, Power MS, Robertson PK, Seed RB, and Stokoe II KH, 2001. Liquefaction Resistance of Soils: Summary Report from the 1996 NCEER and 1998 NCEER/NSF Workshops on Evaluation of Liquefaction Resistance of Soils. *Journal of Geotechnical and Geoenvironmental Engineering* 2001; **124**(10).

Boroschek R, Soto P, and León R. *Registros del Terremoto del Maule, Mw=8.8, 27 de Febrero de 2010*. RENADIC Report 10/05 2010.

ATC/MCEER Joint Venture. *Recommended LRFD guidelines for the seismic design of highway bridges.* Liquefaction Study Report No. MCEER/ATC-49-1 Prepared under NCHRP Project 12-49, Applied Technology Council, Multidisciplinary Center for Earthquake Engineering Research, Buffalo, N.Y 2003.

Ledezma C. and Bray J. Probabilistic Performance-Based Procedure to Evaluate Pile Foundations at Sites with Liquefaction-Induced Lateral Displacement. *Journal of Geotechnical and Geoenvironmental Engineering* 2010; **136**(3): 464–476.

Bray JD and Travasarou T. Simplified procedure for estimating earthquake-induced deviatoric slope displacements. *Journal of Geotechnical and Geoenvironmental Engineering* 2007; **133**(4): 381–392.

Bellana N. *Shear wave velocity as function of SPT penetration resistance and vertical effective stress at California bridge sites.* (Master degree thesis) M.Sc. Civil and Environmental Engineering, University of California, Los Angeles 2009.

Reese L C, Cox WR, and Koop FD. Analysis of Laterally Loaded Piles in Sand. Proceedings, *6th Offshore Technology Conference* 1974; **2**: 473-484.

O'Neill MW and Murchison JM. *An Evaluation of p-y Relationships in Sands*. Report to the American Petroleum Institute, PRAC 82-41-1, The University of Houston-University Park, Houston 1983.

Rollins KM, Gerber TM, Lane JD and Ashford SA. Lateral Resistance of a Full-Scale Pile Group in Liquefied Sand. *Journal of the Geotechnical and Geoenvironmental Engineering Division*, ASCE 2005a; **131**: 115-125.

Matlock H. Correlations for Design of Laterally Loaded Piles in Soft Clay. *Proceedings, 2nd Offshore Technology Conference* 1970; 1: 577-594.